The EMBO Journal Vol.18 No.20 pp.5540–5547, 1999

Oncogenic potential of EAG K^+ channels

Luis A.Pardo[1], Donato del Camino[2], Araceli Sánchez, Frauke Alves[3], Andrea Brüggemann[4], Synnöve Beckh and Walter Stühmer

Max-Planck-Institut für experimentelle Medizin, Hermann-Rein-Strasse 3, D-37075 Göttingen and [3]Abteilung Hämatologie und Onkologie, Universitätsklinikum Göttingen, Göttingen, Germany

[2]Present address: Neurobiology Department, Harvard Medical School, Boston, MA 02115, USA
[4]Present address: Hoechst-Marion-Roussel, DG Cardiovascular, H821, D-65926 Frankfurt, Germany

[1]Corresponding author
e-mail: pardo@mail.mpiem.gwdg.de

We have investigated the possible implication of the cell cycle-regulated K^+ channel *ether à go-go* (EAG) in cell proliferation and transformation. We show that transfection of EAG into mammalian cells confers a transformed phenotype. In addition, human EAG mRNA is detected in several somatic cancer cell lines, despite being preferentially expressed in brain among normal tissues. Inhibition of EAG expression in several of these cancer cell lines causes a significant reduction of cell proliferation. Moreover, the expression of EAG favours tumour progression when transfected cells are injected into immune-depressed mice. These data provide evidence for the oncogenic potential of EAG.
Keywords: *ether à go-go*/K^+ channels/proliferation/transformation

Introduction

Ether à go-go (EAG) K^+ channels were first cloned from *Drosophila melanogaster* (dEAG; Warmke *et al.*, 1991) and functionally expressed in *Xenopus* oocytes (Brüggemann *et al.*, 1993). Mammalian EAG channels have been cloned and expressed from rat brain (rEAG; Ludwig *et al.*, 1994), mouse brain (mEAG; Warmke and Ganetzky, 1994; Robertson *et al.*, 1996) and bovine retina (bEAG; Frings *et al.*, 1998). Together they form a family whose mammalian members share >85% homology in their DNA sequence (Warmke and Ganetzky, 1994).

The first attempts to clone a human EAG led to the discovery of *HERG* (human eag-related gene; Warmke and Ganetzky, 1994). Recently, Meyer and Heinemann (1998) electrophysiologically described a current highly reminiscent of EAG in SH-SY5Y human neuroblastoma cells, and a human EAG has been cloned from myoblasts (Occhiodoro *et al.*, 1998).

Pharmacological evidence indicates that K^+ channels might be involved in the cell cycle and proliferation. A well-documented case of the role of K^+ channels in proliferation and differentiation stems from lymphocytes (e.g. DeCoursey *et al.*, 1984), although it has also been shown in several other cell types, such as breast cancer cells (e.g. Strobl *et al.*, 1995), brown fat cells (Pappone and Ortiz-Miranda, 1993), melanoma cells (Nilius and Wohlrab, 1992), keratinocytes (Mauro *et al.*, 1997), prostate cancer cells (Skryma *et al.*, 1997) and Schwann cells (Pappas and Ritchie, 1998). The role of K^+ channels in these cellular events has traditionally been explained by either the possible influence of K^+ channels on the intracellular Ca^{2+} concentration (a known effector of cell differentiation and proliferation; e.g. Santella, 1998), or, alternatively, the control of cell volume via K^+ channels (Rouzaire-Dubois and Dubois, 1998). The role of K^+ channels in proliferation is indirect in both mechanisms.

Several indications allow us to propose a direct involvement of EAG channels in the cell cycle. We have demonstrated recently that rEAG K^+ channels are modulated during the paradigmatic example of relief from cell cycle arrest: maturation of *Xenopus* oocytes (Brüggemann *et al.*, 1997); the modulation consists of a profound change in the permeation properties of the channel (Pardo *et al.*, 1998). These findings, together with the observations presented in this work (transformation ability, ectopic expression in cancer cells and a role favouring tumour progression *in vivo* for EAG channels) suggest a role of EAG in controlling the cell cycle and/or cell proliferation.

Results

Transforming activity of EAG

The first indication of a possible role of EAG in cell proliferation and growth came from its modulation during cell cycle-related events (Brüggemann *et al.*, 1997; Pardo *et al.*, 1998). To address the question of whether or not this modulation is related to a role of EAG in the cell cycle and proliferation, we compared the growth of rEAG-expressing (Ludwig *et al.*, 1994) CHO cells (CHOrEAG) with cells expressing a rat voltage-dependent K^+ channel, rKv1.4 (CHOKv), and with wild-type cells. Figure 1 shows the data for one of the three independent clones of CHOrEAG cells tested and for wild-type cells. CHOKv cells showed essentially identical behaviour to wild-type, and all clones of CHOrEAG cells were indistinguishable from each other in these experiments. The growth rate was quantified using the MTT assay (Mosmann, 1983). Metabolic activity in CHOrEAG cells was significantly higher (Figure 1A, circles) than in wild-type cells (triangles). It is important to point out that the cells were maintained without changing the medium for the duration of the experiment. This might offer an alternative interpretation of the results, namely that the medium is able to support the growth of a larger number of CHOrEAG cells. Consistent with this interpretation, conditions that do not support the growth of wild-type cells (0.5% fetal

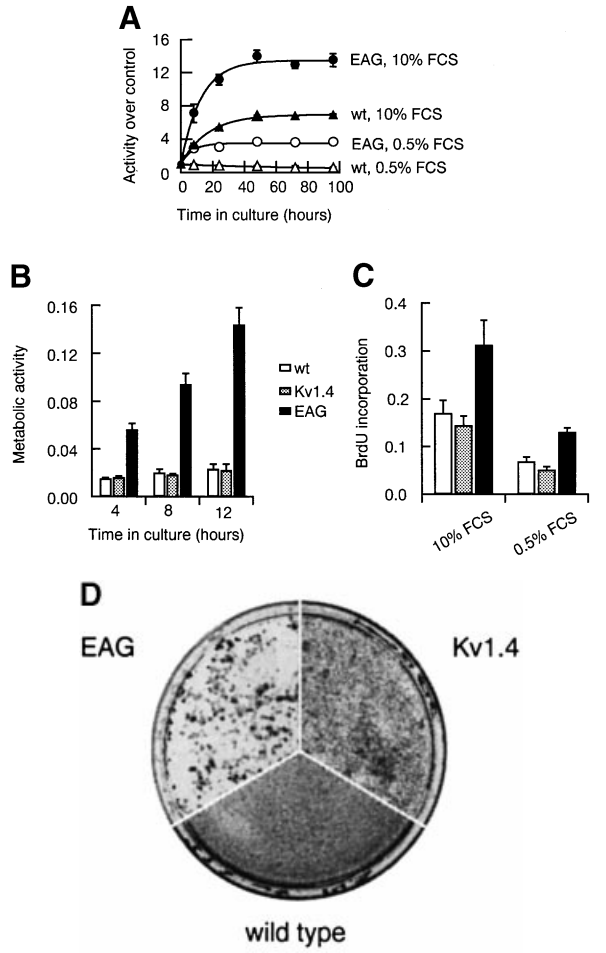

Fig. 1. Transformed phenotype of rEAG-transfected CHO cells. (**A**) Growth curves of CHO cells transfected with rEAG (circles) as compared with naive cells (triangles) in 10% (filled symbols) or 0.5% (open symbols) fetal calf serum (FCS). The values represent the mean ± SEM of eight determinations. (**B**) Increase in metabolic activity during the first 12 h after removal of S-phase block. (**C**) DNA increase after removal of S-phase block for a 12 h incubation in 10% FCS or a 24 h incubation in 0.5% FCS. The bars represent the mean ± SD. (**D**) Foci formation of rEAG-transfected NIH 3T3 cells compared with cells transfected with rKv1.4 and with wild-type cells.

calf serum instead of 10%; see Figure 1A, open symbols) do allow the growth of CHOrEAG cells for at least two population doublings.

Such an increase in metabolic activity measured by MTT hydrolysis could also be due to factors other than proliferation. To test the effects of EAG on cell proliferation more directly, DNA synthesis was measured by incorporation of 5-bromo-deoxyuridine (BrdU) in cells synchronized in the S phase of the cell cycle by means of thymidine arrest (Stein *et al.*, 1995). Consistent with our previous findings, when the S phase of the cell cycle was allowed to proceed by reduction of the thymidine concentration, CHOrEAG cells showed higher metabolic activity (Figure 1B) and increased BrdU incorporation (Figure 1C). These results suggest that more EAG-transfected cells entered the S phase during the thymidine treatment and/or DNA synthesis was elevated, in any case indicating a faster proliferation rate in CHOrEAG cells. In the presence of a low concentration of serum, BrdU incorporation was also significantly higher in CHOrEAG than in wild-type cells (Figure 1C).

A further indication of transformation is loss of contact inhibition (Jainchill *et al.*, 1969). Figure 1D shows that NIH 3T3 cells transiently transfected with the rEAG channel continued growing into foci, while wild-type and rKv1.4-transfected control cells ceased growing once a homogeneous monolayer covered the plate. NIH 3T3 cells are also substratum-dependent and fail to proliferate in a semi-solid medium containing 0.3% agar (Hermouet *et al.*, 1991). However, rEAG- (but not rKv1.4-) transfected cells formed colonies under such conditions, regardless of the vector used for transfection. The number of colonies >0.1 mm in diameter per microgram of DNA used for transfection was determined using automated image processing after 14 days in a medium containing 0.3% agar. Cells transfected with rEAG in pTracer or pcDNA3 gave rise to 9.9 ± 2.4 or 8.5 ± 3.2 colonies/μg DNA, while transfection with Kv1.4 in the same vectors gave 0 or 1.4 ± 0.7 colonies/μg DNA, respectively. Control transfections with GFP in pcDNA3 or transfection buffer gave <1 colony per microscope field. All of the above results indicate a transforming potential of EAG.

Cloning of human EAG (hEAG)

Proliferation of human breast carcinoma MCF-7 cells has been shown to be sensitive to treatment with several potassium channel blockers (Woodfork *et al.*, 1995). Since the drugs used to inhibit the proliferation of MCF-7 cells also inhibit EAG currents (see for example Brüggemann *et al.*, 1993), we searched for the presence of EAG currents in MCF-7 cells. Using the patch–clamp technique, we found a voltage-dependent current compatible, in terms of conductance and voltage-dependence, with EAG. These currents were blocked by astemizole, a known blocker of HERG channels (Suessbrich *et al.*, 1996) that also blocks rEAG (A.Brüggemann and L.A.Pardo, unpublished). By means of PCR with degenerate ODNs, we were able to isolate the complete open reading frame for hEAG from a human brain library (but not from a human mammary gland library). Our sequence is identical at the amino acid level to the one reported by Occhiodoro and co-workers, which they isolated from human myoblasts (Occhiodoro *et al.*, 1998).

Two alternatively spliced variants have been described for the mouse and bovine channel (Warmke and Ganetzky, 1994; Frings *et al.*, 1998). We isolated a phage containing a partial sequence identical to hEAG, but with an 81 bp insertion at position 951 that corresponds to the long splice variant, hEAGb. hEAGb contains an additional 27 amino acids between transmembrane segments S3 and S4 with total amino acid identity between mouse, bovine and human EAG. Also, RT–PCR on human brain RNA with ODNs specifically designed to amplify both splice variants revealed the existence of two bands with the expected sizes of hEAGa and hEAGb.

Chromosomal localization of hEAG

The chromosomal localization of the *hEAG* gene was determined by fluorescence *in situ* hybridization (FISH) with a biotinylated probe comprising 1.5 kbp of the 3′ end of the *hEAG* open reading frame and 2.5 kbp of 3′-untranslated region. Two regions of one chromosome were positive. Under the conditions used, the hybridization efficiency was ~87% for this probe (among 100 checked

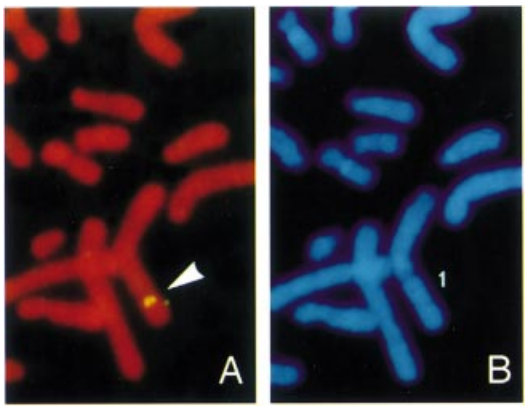

Fig. 2. Example of FISH mapping of hEAG. (**A**) FISH signals on chromosome (arrowhead). (**B**) The same mitotic figure stained with DAPI to identify chromosome 1.

mitotic figures, 87 of them showed signals on one pair of chromosomes). The assignment between the signal from that probe and the long arm of chromosome 1 was obtained using 4′-6-diamidine-2-phenylindole (DAPI) banding. The detailed position was further delimited based on the summary from 10 photographs, whereby the *hEAG* gene is located at position 32.1–32.3 of the long arm of human chromosome 1 (Figure 2).

Expression pattern of hEAG

The expression of hEAG mRNA in various tissues was assayed using Northern blot analysis as well as dot-blot and single-tube RT–PCR. In the first case, a strong hybridization signal of ~9.2 kb was detected in brain and a faint signal of similar size in placenta, whereas heart, lung, liver, skeletal muscle, kidney and pancreas were negative even after long exposures (not shown).

Dot-blot analysis of mRNAs from a number of adult (spinal cord, heart, aorta, skeletal muscle, colon, bladder, uterus, prostate, stomach, testis, ovary, pancreas, pituitary gland, thyroid gland, salivary gland, mammary gland, kidney, liver, small intestine, spleen, thymus, peripheral leukocyte, lymph node, bone marrow, appendix, lung, trachea and placenta) and fetal tissues (brain, heart, kidney, liver, spleen, thymus and lung) also failed to detect expression of hEAG, except in adult brain. Of the brain areas investigated, only substantia nigra, thalamus and medulla oblongata were negative, whereas amygdala, caudate nucleus, cerebral cortex, cerebellum, putamen, hippocampus, frontal lobe, occipital lobe, temporal lobe and subthalamic nucleus showed positive signals (not shown).

In addition, total RNA from human brain, heart, trachea, adrenal gland, liver, kidney, skeletal muscle and mammary gland, and spinal cord poly(A)$^+$ RNA, as well as total RNA from the adenovirus-transformed line 293 (as a human non-tumoral cell line) were analysed by RT–PCR to amplify fragments of both hEAG splice variants. PCR products were analysed by Southern blot using a 980 bp hEAG probe. The integrity of RNA was assessed by parallel amplification of a transferrin receptor (TFR) fragment. Among all RNAs tested, hEAG a and hEAG b fragments were amplified only in brain (Figure 3A).

As discussed above, the expression of hEAG is confined to brain and possibly placenta, but the original cDNA

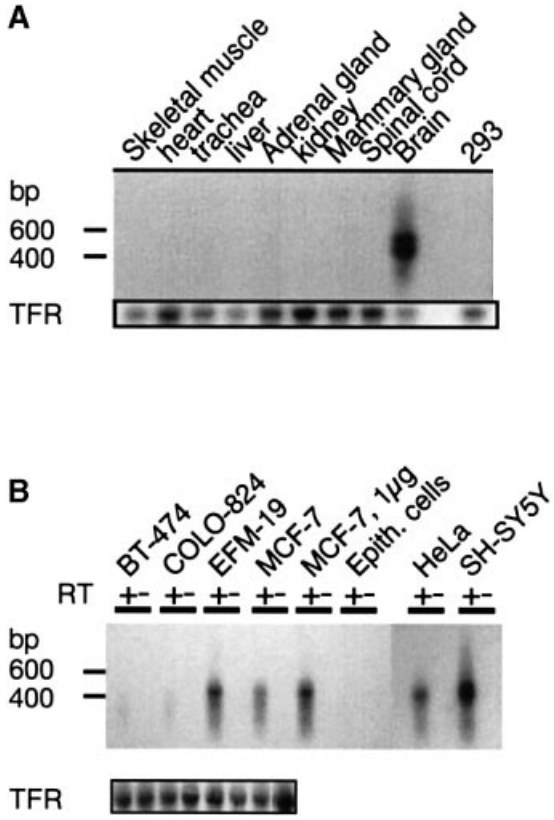

Fig. 3. Southern blots of RT–PCR products of the indicated RNAs hybridized with a hEAG probe. (**A**) The two bands corresponding to hEAGa and hEAGb could be amplified and identified under our experimental conditions only in brain. (**B**) Among the different human cell lines and mammary epithelial cells in primary culture analysed, only the latter are clearly negative. Transferrin receptor (TFR) signals are shown at the bottom of each gel.

fragment was obtained from MCF-7 cells, a tumour cell line of breast origin. In addition, we were unable to detect hEAG in normal human breast RNA, indicating that hEAG is present in the cell line but not in normal mammary gland. This observation raises the question of whether or not other tumour cell lines express hEAG. To investigate this, we prepared RNA from several other cell lines and tested for hEAG expression by RT–PCR (Figure 3B): HeLa (carcinoma of the cervix), SH-SY5Y (neuroblastoma), and in particular lines from mammary gland tumours: COLO-824 (carcinoma), EFM-19 (carcinoma), BT-474 (ductal carcinoma), together with MCF-7 cells and normal brain as positive controls. Total RNA from cultured mammary gland epithelial cells was included to circumvent the mixed cell populations in whole mammary gland. In HeLa, SH-SY5Y, EFM-19 and MCF-7 RNA, a hEAG band could be amplified, whereas the signal obtained in RNA from COLO-824 and BT-474 was too weak to allow these lines to be considered as positive. Cultured epithelial cells, as well as the 293 cells (Figure 3A), were negative.

Inhibition of tumour cell proliferation by hEAG-specific antisense ODNs

Is the expression of hEAG in some tumour cells just the consequence of their abnormal growth, or is this K^+ channel necessary for their proliferation? In the latter case, inhibition of hEAG expression with antisense

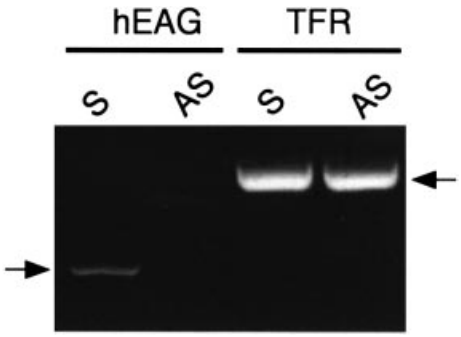

Fig. 4. Reduction of hEAG RT–PCR product levels of RNA from EFM-19 cells treated with 1 μM antisense ODN (AS) and control (sense ODN-treated) cells (lanes S). TFR signals did not decrease. The arrows indicate the expected sizes of the fragments.

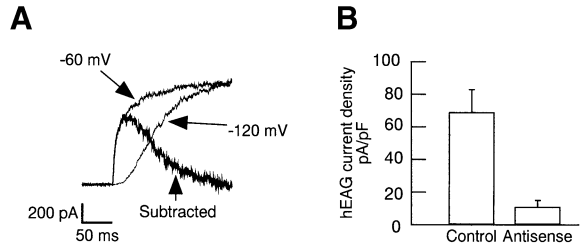

Fig. 5. (**A**) Current traces measured from an SH-SY5Y cell after depolarization to +60 mV from either –120 or –60 mV. The first part of the subtracted trace corresponds to the isolated EAG current. (**B**) Current density in SH-SY5Y cells treated with antisense ODNs was significantly reduced as compared with control cells. Mean ± SEM for 9 (control) or 25 (antisense) cells.

oligonucleotides (ODNs) should decrease the proliferation rate of these tumour cells.

We tested the efficiency of the antisense ODN treatment in reducing the hEAG mRNA content in EFM19 cells (Figure 4). The cells were incubated overnight with 1 μM antisense ODN and total RNA was prepared and tested for the presence of hEAG by single-tube RT–PCR. A significant reduction in the amount of PCR product was detected as compared with the control (sense) ODN. Similar results were obtained with MCF-7 and SH-SY5Y cell lines.

To test the ability of the antisense ODN also to reduce hEAG activity functionally, we studied hEAG-mediated K^+ currents in SH-SY5Y cells treated with antisense ODN (Figure 5). To isolate hEAG currents, we took advantage of the peculiar voltage-dependence of activation shown by all known mammalian EAGs, including hEAG (Terlau *et al*., 1996; Bijlenga *et al*., 1998). The time constant of activation is strongly influenced by the voltage prior to the stimulus (holding voltage, V_{hold}). This means that the current activates very slowly when V_{hold} is very negative (e.g. –120 mV) and much faster at less hyperpolarized V_{hold} (e.g. –60 mV). We stimulated the cells for 200 ms to +60 mV, starting from V_{hold} of either –120 or –60 mV, and then subtracted both traces (Figure 5A). In any 'typical' non-inactivating K^+ channel, this subtraction would result in no current. In hEAG, however, during the first tens of milliseconds both pulses diverge strongly: a current is seen at –60 mV that is not yet activated at –120 mV. After this initial time, the current amplitudes approach each other progressively and finally merge. Under our experimental conditions, the maximal difference

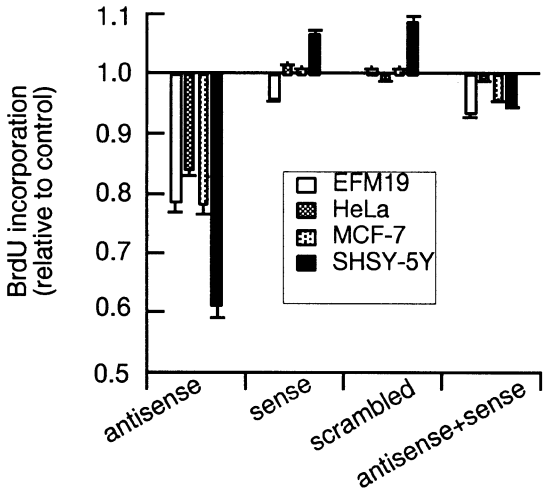

Fig. 6. Inhibition of DNA synthesis in human cancer cells (EFM-19, HeLa, MCF-7 and SH-SY5Y) by antisense ODNs directed against hEAG. DNA synthesis is expressed relative to BrdU incorporation in the absence of ODNs. The bars indicate the mean ± SD for eight wells per condition in a representative experiment.

arises 20 ms after the start of the stimulus. The effect of antisense ODN on the magnitude of this difference relative to the total cell surface (expressed as capacity) is depicted in Figure 5B. A strong reduction in hEAG current was already observed 24 h after antisense treatment, indicating that the antisense ODN treatment not only reduces the RNA content but also the functional protein present in the membrane of these cells.

Figure 6 shows results obtained on the proliferation of EFM-19, HeLa, MCF-7 and SH-SY5Y cells. There was a significant reduction of DNA synthesis in cultures treated with antisense ODNs only ($p < 0.0001$ in Student's *t*-test). Equivalent results were obtained when the metabolic activity of viable cells was measured by the MTT assay (data not shown). To discard non-specific ODN effects, we performed controls (Wagner, 1994) using either scrambled, sense ODN or the antisense ODN in the presence of an excess of sense ODN. Growth of cultures treated with sense, scrambled or double-stranded ODNs was comparable to that of untreated control cultures ($p > 0.1$). These results suggest that hEAG expression might play a role in the proliferation of these cancer cell lines.

Tumour progression in SCID mice

To determine whether the expression of hEAG is advantageous for tumour cells *in vivo*, we performed subcutaneous implants of CHO cells expressing the channel (CHOhEAG) into the flank of female, severe combined immune-deficient (SCID) mice (Bosma *et al*., 1983). CHOKv cells (see above) were used as a control. One week after the implantation, all CHOhEAG-injected mice carried tumours detectable by palpation, while no mass >1 mm was observed in the controls; this latter observation correlates well with previous reports where similar numbers of CHO cells were implanted (e.g. Ferrara *et al*., 1993; Richter *et al*., 1993). During the second week post-implantation, the hEAG-expressing tumours reached diameters in excess of 5 mm and visibly emerged through the skin in most cases (Figure 7A); the mice were killed after 2 ($n = 6$) or 3 ($n = 7$) weeks. All CHOhEAG-injected animals showed tumours.

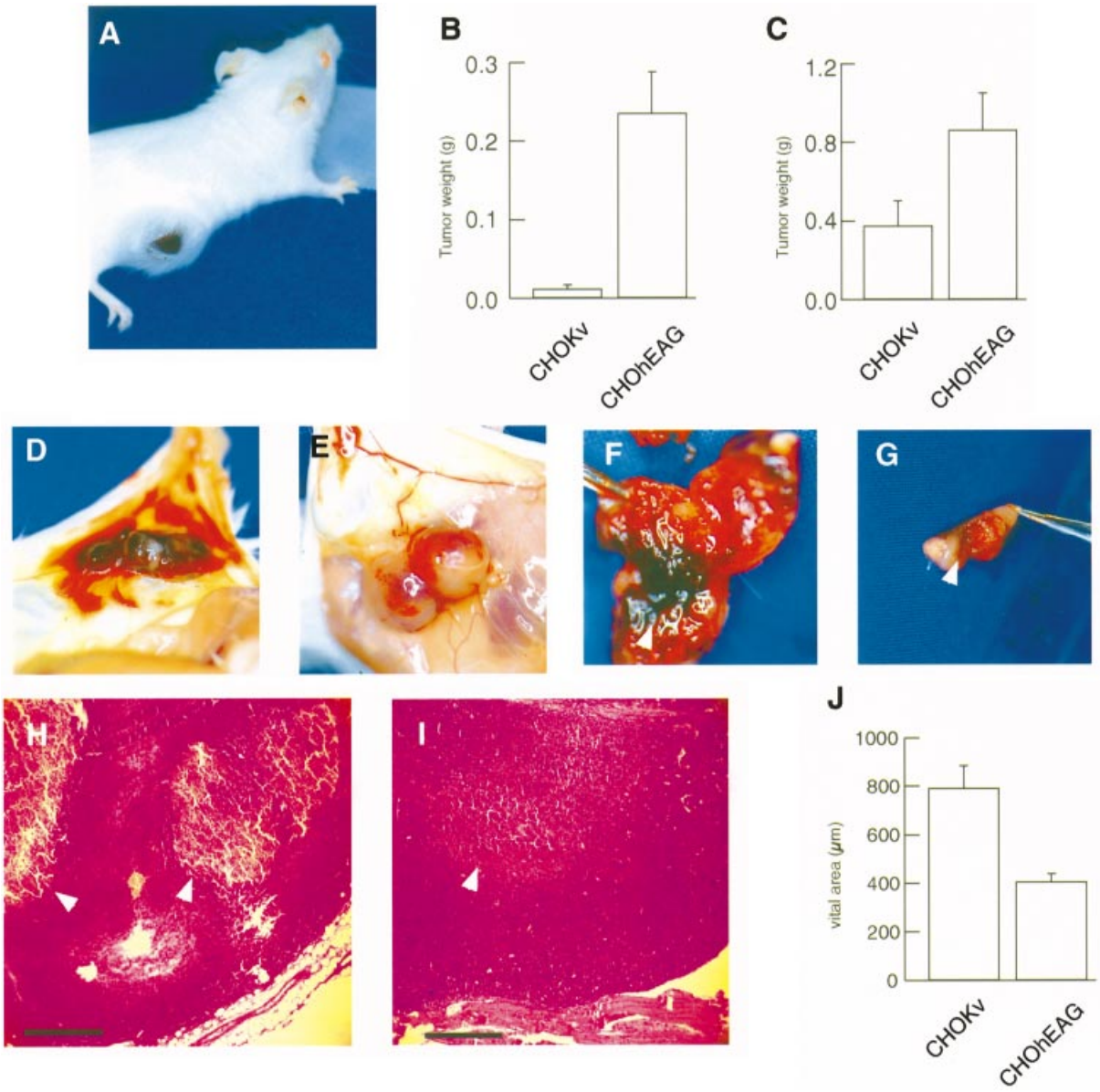

Fig. 7. hEAG expression favours tumour progression. (**A**) Subcutaneous implantation of CHOhEAG cells induced aggressive tumours that grew rapidly and soon broke the skin of the carrier mice (third week post-implantation). (**B** and **C**) The average mass of CHOhEAG tumours was significantly greater than that of the CHOKv tumours both 2 weeks (B; mean ± SEM; $p = 0.002$) and 3 weeks (C; mean ± SEM; $p = 0.03$) post-implantation. (**D**) CHOhEAG and (**E**) CHOKv tumours photographed *in situ*. (**F**) CHOhEAG and (**G**) CHOKv tumours cut open to show the great extent of necrosis (arrowheads) in the former. (**H** and **I**) A greater degree of necrosis and fixation to the skin in CHOhEAG tumours (H) are also evident microscopically after paraffin embedding and haematoxylin–eosin staining. The histology is comparable in both micrographs, but in (H) a much larger necrotic area is observed (arrowheads). Scale bars in (H) and (I), 100 μm. (**J**) The average width of the vital area in CHOKv tumours was significantly larger than that of CHOhEAG tumours (mean ± SEM; $p < 0.0005$).

The average mass (Figure 7B and C) of the hEAG-expressing tumours was significantly greater than that of controls, especially 2 weeks following implantation (Figure 7B). From macroscopic observation, the tumours appeared friable and haemorrhagic; the CHOhEAG tumours were darker than the controls and were adhered to the skin (Figure 7D and E) in all CHOhEAG-injected mice at 2 weeks. In contrast, the tumour could be easily dissected from the skin in all of the control mice after 2 weeks and in five out of six mice at 3 weeks. The tissue below the tumour appeared unaffected in all cases. The dark colour was due to a great extent of intratumour necrosis (Figure 7F and G, arrowheads), confirmed by histology (Figure 7H and I, arrowheads). Accordingly, the thickness of the vital area in the EAG-expressing tumours was significantly smaller than in the controls (Figure 7J).

Intratumoral necrosis is a frequent finding in tumours with rapid growth; if the tumour grows faster than the vascular network, the blood supply will not be sufficient to sustain its growth. The rapid growth of the tumour can thus account for the massive intratumoral necrosis observed in the CHOhEAG group. We attribute the relative stagnation of growth of the CHOhEAG tumours after 3 weeks of implantation to this massive necrosis. These

data strongly suggest that expression of hEAG represents an advantage for the proliferation of tumour cells *in vivo*, since CHOhEAG tumours grow faster and are more aggressive than CHOKv tumours.

Discussion

Overexpression of rEAG potassium channels in CHO or NIH 3T3 cells induces significant features characteristic of malignant transformation, such as faster growth, loss of growth factor- and substrate-dependence, and loss of contact inhibition. Moreover, hEAG is expressed ectopically in human cancer cell lines and expression of hEAG represents an advantage for the progression of tumours in SCID mice *in vivo*. These findings, together with the strong modulation of EAG channels during the cell cycle, strongly suggest a direct involvement of EAG channels in cell proliferation and prompt the possibility of participation of the protein in the pathogenesis of some tumours. This hypothesis is additionally supported by results reported recently from myoblasts (Bijlenga *et al.*, 1998; Occhiodoro *et al.*, 1998), since hEAG is expressed over a short time frame immediately preceding myoblast fusion, a proliferation-related phenomenon. A possibility that arises from the data presented is that given a role of EAG channels in proliferation, the abnormal expression and/or regulation of the channel may induce pathological proliferation, either degeneration or tumour growth.

The restricted expression of the hEAG transcript, not surprising in itself for a K^+ channel, was intriguing for us since we had isolated our first cDNA from an epithelial tumour cell line (MCF-7), not from brain tissue. When other cancer cell lines were tested, we found high expression levels of hEAG in EFM-19, SH-SY5Y and HeLa cells, tumour cell lines of diverse origin. Since two breast cancer cell lines were clearly positive for hEAG expression, we analysed the expression in normal breast and also in cultured primary mammary gland epithelial cells to avoid the contribution of a mixed cell population. The absence of any specific signal supports the idea of a tumour-specific expression of hEAG. In these cell lines, inhibition of hEAG expression by antisense ODNs leads to a reduction of DNA synthesis.

Our results with SCID mice also indicate that expression of hEAG offers an advantage for the growth of tumour cells, since CHOhEAG tumours show faster growth and are more aggressive than CHOKv tumours.

HERG K^+ channels have also been reported to show differential expression patterns in tumour cell lines. Overexpression of HERG has been suggested to represent a selective advantage for these tumour cells (Bianchi *et al.*, 1998), although HERG is expressed in many normal tissues. It is noteworthy that this other member of the same family is also related to proliferation and/or differentiation to some extent, but there has been no report showing transforming activity for HERG.

Overexpression of a K^+ channel is expected to alter the resting potential of cells. This is indeed the case for overexpression of EAG in CHO cells. We do not think that this alteration alone is responsible for the effects observed, since CHOKv cells do not show altered growth properties, although their resting potential is also more negative than that of wild-type cells. It is tempting to speculate that the modulation of EAG current during the cell cycle (Brüggemann *et al.*, 1997; Pardo *et al.*, 1998) plays a crucial role in the transforming properties of the channel.

In summary, our results not only demonstrate the transforming activity of EAG and its ectopic expression in several tumour cell lines, but also strongly suggest an involvement of hEAG in the proliferation of those cells. The study of a larger number of cell lines and tumours will certainly provide information on the possible diagnostic and/or prognostic value of hEAG expression.

Materials and methods

Cell lines

All human cell lines—293 (DSMZ ACC 305), adenovirus-transformed primary embryonic kidney; BT-474 (DSMZ ACC64), breast invasive ductal carcinoma; CHO-K1 (DSMZ ACC 110); COLO-824 (DSMZ ACC 200), breast carcinoma; EFM-19 (DSMZ ACC 231), breast carcinoma, ductal type; HeLa (DSMZ ACC 57), carcinoma of the cervix; MCF-7 (DSMZ ACC 115), breast adenocarcinoma; NIH-3T3 (DSMZ ACC 59); and SH-SY5Y (DSMZ ACC 209), neuroblastoma—were obtained from Deutsche Sammlung von Mikroorganismen und Zellkulturen (DSMZ) and maintained following the DSMZ catalogue guidelines. Normal human mammary epithelial cells were purchased from BioWhittaker.

Transfection and proliferation studies

Transient transfection was carried out following the calcium phosphate method described previously (Chen and Okayama, 1987). Cell lines were established by selection through the G-418 resistance encoded in the pcDNA3 vector. For proliferation assays, cells were plated at a density of 10^4 cells/ml and MTT (Mosmann, 1983; 0.5 mg/ml) was added to the cultures at the time points indicated. Four hours later, the product was solubilized and the reaction stopped using 10% SDS in 0.01 M HCl. After overnight incubation, the colour produced was read at 562 nm (reference 650 nm).

To test the formation of foci, cells transfected with pcDNA3 (control) or with the same vector carrying either the rEAG or the Kv1.4 sequences were maintained in rich medium until the control cells reached confluence. The plates were then fixed with methanol and stained with Giemsa blue. Colony formation experiments were carried out by plating the transfected cells in regular medium containing 0.3% agar onto a layer containing 0.55% agar. Colonies >0.1 mm in diameter were scored 14 days after transfection (Hermouet *et al.*, 1991).

Cloning of hEAG

Degenerated ODN primer pairs were designed to amplify a DNA fragment of hEAG by PCR using cDNA from MCF-7 cells as a template. For the design of the ODNs, special thought was given to avoiding the amplification of HERG, which is also expressed in these cells. Using these ODNs, we amplified the expected 400 bp fragment of hEAG with a sequence $>80\%$ identical at the DNA level and $>90\%$ identical at the amino acid level to rEAG. We then used this fragment as a probe to screen a human cDNA library. We did not use an MCF-7 cell library, since cancer cells might carry mutations. However, we did not obtain any positive signals from a normal human breast cDNA library. Furthermore, PCR using specific primers designed from the 400 bp fragment isolated from MCF-7 cells failed to amplify any fragments using the breast cDNA library as a template. However, under identical conditions the same ODNs amplified two bands from a human brain cDNA library. We then screened this library and succeeded in isolating the full-length open reading frame for hEAG. Although we did not find a stop codon in-frame upstream of the putative initiating methionine, position 1 was assigned based on sequence homology to the other mammalian EAGs.

The procedure of FISH for chromosomal localization was performed according to Heng *et al.* (1992) and Heng and Tsui (1993).

RT–PCR, Northern blot and dot-blot analysis

Total RNA was isolated from all cell lines listed following the protocol described previously (Chomczynski and Sacchi, 1987). Single-tube RT–PCR on RNAs from the different cell lines and on commercial RNAs from the following human tissues (all from Clontech): total RNA from

brain, liver, heart, skeletal muscle, adrenal gland, lung, trachea and kidney, and poly(A)$^+$ RNA from spinal cord, was performed as described previously (Soto *et al.*, 1996) with an annealing temperature of 63°C. Primer sequences were as follows. Forward: 5′-CGCATGAACTA-CCTGAAGACG (position 862–882); reverse: 5′-TCTGTGGATGG-GGCGATGTTC (position 1340–1320). The expected DNA length is 479 bp for hEAGa and 560 bp for hEAGb. Specific primers for TFR, forward: 5′-TCAGCCCAGCAGAAGCATTAT and reverse: 5′-CTG-GCAGCGTGTGAGAGC, were used as a control of RNA and PCR performance. These ODNs were designed according to the published TFR sequence (McClelland *et al.*, 1984; Schneider *et al.*, 1984), starting at exon 11 and spanning to exon 19 (Evans and Kemp, 1997). The 806 bp product was amplified in parallel reactions as expected. The DNA fragment from brain was cloned into pGEM-T vector and used as a probe in Southern blot analysis for all other RNAs. The amplification of genomic DNA was ruled out by the use of ODNs spanning at least an intron for all amplifications (the product from genomic DNA would then be bigger than the one from cDNA) and with amplification in the absence of reverse transcription. Standard controls without RNA were performed to discard contaminant DNA.

Aliquots (50 µl hEAG or 15 µl TFR) of the PCRs were analysed in 2% agarose gels. The DNA was transferred to membranes and hybridized at high stringency with the corresponding [^{32}P]dCTP-labelled random primed probe, consisting of either a 980 bp hEAG fragment (position 277–1257) or the TFR fragment obtained from brain.

A human multiple tissue Northern blot (Clontech 7760-1) was hybridized with the 705 bp [^{32}P]dCTP-labelled hEAG fragment (position 1258–1963) following the accompanying protocol. After the final washing step (0.1× SET, 0.1% SDS, 65°C for 60 min), a phosphoimager plate was exposed for 60 min and subsequently read. A dot-blot membrane (Clontech MasterBlot) was hybridized with the same probe, using the manufacturer's recommended protocol, washed and read in a phosphoimager for 3 h.

Antisense assays

A 19mer antisense phosphorothioate ODN (5′-CAGCCATGGTCAT-CCTCCC) spanning the putative initiation codon of hEAG was used to test proliferation inhibition. The sense ODN and a scrambled sequence (GTCGGTACCAGTAGGAGGG) were used as controls. We had optimized the uptake conditions into cells using fluorescein-labelled antisense ODN. Cells were seeded in 96-well plates at a density of 10^5 cells/ml. One day after plating, the cells were washed with culture medium and the ODN was added (final concentration 10 µM). The ODN had previously been mixed with 20 µg/ml of the transfection reagent DAC-30 (Eurogentec) in serum-free medium and allowed to incubate at room temperature for 20–30 min. The mixture was then added as a 1:1 dilution in culture medium and maintained in contact with cells overnight. After this incubation, the cells were washed and labelled with BrdU (100 µM) for 2 h. Incorporation was detected using the kit from Boehringer Mannheim. The electrophysiological determinations were performed using standard protocols in the whole-cell configuration of the patch–clamp technique (Hamill *et al.*, 1981) with an extracellular solution containing (mM) 140 NaCl, 2.5 KCl, 2 $CaCl_2$, 2 $MgCl_2$, 10 HEPES–NaOH pH 7.2, 10 glucose. The pipette solution was (mM) 140 KCl, 10 1,2-bis(2-aminophenoxy)ethane-*N*,*N*,*N*′,*N*′-tetraacetic acid, 10 HEPES–KOH pH 7.2.

In vivo tumour progression

A total of 2×10^6 CHO-hEAG or CHO-Kv1.4 cells suspended in 100 µl phosphate-buffered saline were implanted subcutaneously on the flank of 6- to 8-week-old female Fox Chase SCID mice (*C.B-17/Icr sicd/scid*) obtained from Bomholtgard, Ry, Denmark. The presence of tumours was checked every second day by tactile inspection of every mouse. Either 2 or 3 weeks after implantation, the animals were killed by cervical dislocation and the tumours dissected and fixed in paraformaldehyde for subsequent paraffin inclusion and staining. The identity of the CHOhEAG cells was established by UV illumination of the fresh tumours (1 mm slices) to evoke fluorescence from the green fluorescent protein encoded in the pTracer vector (Invitrogen).

Accession numbers

DDBJ/EMBL/GenBank accession Nos for the sequences reported in this paper are AF078741 (hEAGa) and AF078742 (hEAGb).

Acknowledgements

We thank Dr F.Soto for invaluable help with the molecular biology experiments, Dr R.Weseloh for helpful discussions, Dr M.Hollmann for the pSGEM vector construct, Dr O.Pongs for the pcDNA3-rEAG and pcDNA3-Kv1.4 constructs, and V.Díaz-Salamanca, B.Scheufler and S.Voigt for expert technical assistance. We acknowledge Dr Henry Heng (SeeDNA Biotech, Downsview, Ontario, Canada) for FISH analysis. During this work, D.d.C. was supported by a Postdoctoral Fellowship from FICYT, Pdo. de Asturias, Spain.

References

Bianchi,L. *et al*. (1998) *HERG* encodes a K^+ current highly conserved in tumors of different histogenesis—a selective advantage for cancer cells? *Cancer Res.*, **58**, 815–822.

Bijlenga,P., Occhiodoro,T., Liu,J.H., Bader,C.R., Bernheim,L. and Fischer-Lougheed,J. (1998) An *ether-á-go-go* K^+ current, $I_{h\text{-}eag}$, contributes to the hyperpolarization of human fusion-competent myoblasts. *J. Physiol.*, **512**, 317–323.

Bosma,G.C., Custer,R.P. and Bosma,M.J. (1983) A severe combined immunodeficiency mutation in the mouse. *Nature*, **301**, 527–530.

Brüggemann,A., Pardo,L.A., Stühmer,W. and Pongs,O. (1993) *Ether-à-go-go* encodes a voltage-gated channel permeable to K^+ and Ca^{2+} and modulated by cAMP. *Nature*, **365**, 445–448.

Brüggemann,A., Stühmer,W. and Pardo,L.A. (1997) Mitosis-promoting factor-mediated suppression of a cloned delayed rectifier potassium channel expressed in *Xenopus* oocytes. *Proc. Natl Acad. Sci. USA*, **94**, 537–542.

Chen,C. and Okayama,H. (1987) High-efficiency transformation of mammalian cells by plasmid DNA. *Mol. Cell. Biol.*, **7**, 2745–2752.

Chomczynski,P. and Sacchi,N. (1987) Single-step method of RNA isolation by acid guanidinium thiocyanate–phenol–chloroform extraction. *Anal. Biochem.*, **162**, 156–159.

DeCoursey,T.E., Chandy,K.G., Gupta,S. and Cahalan,M.D. (1984) Voltage-gated K^+ channels in human T lymphocytes: a role in mitogenesis? *Nature*, **307**, 465–468.

Evans,P. and Kemp,J. (1997) Exon/intron structure of the human transferrin receptor gene. *Gene*, **199**, 123–131.

Ferrara,N., Winer,J., Burton,T., Rowland,A., Siegel,M., Phillips,H.S., Terrell,T., Keller,G.A. and Levinson,A.D. (1993) Expression of vascular endothelial growth factor does not promote transformation but confers a growth advantage *in vivo* to Chinese hamster ovary cells. *J. Clin. Invest.*, **91**, 160–170.

Frings,S., Brull,N., Dzeja,C., Angele,A., Hagen,V., Kaupp,U.B. and Baumann,A. (1998) Characterization of *ether-à-go-go* channels present in photoreceptors reveals similarity to I-kx, a K^+ current in rod inner segments. *J. Gen. Physiol.*, **111**, 583–599.

Hamill,O.P., Marty,A., Neher,E., Sakmann,B. and Sigworth,F.J. (1981) Improved patch–clamp techniques for high-resolution current recording from cells and cell-free membrane patches. *Pflügers Arch.*, **391**, 85–100.

Heng,H.H. and Tsui,L.C. (1993) Modes of DAPI banding and simultaneous *in situ* hybridization. *Chromosoma*, **102**, 325–332.

Heng,H.H., Squire,J. and Tsui,L.C. (1992) High-resolution mapping of mammalian genes by *in situ* hybridization to free chromatin. *Proc. Natl Acad. Sci. USA*, **89**, 9509–9513.

Hermouet,S., Merendino,J.J.,Jr, Gutkind,S. and Spiegel,A.M. (1991) Activating and inactivating mutations of the α subunit of the G_{i2} protein have opposite effects on proliferation of NIH-3T3 cells. *Proc. Natl Acad. Sci. USA*, **88**, 10455–10459.

Jainchill,J.L., Aaronson,S.A. and Todaro,G.J. (1969) Murine sarcoma leukemia virus: assay using clonal lines of contact inhibited cells. *J. Virol.*, **4**, 549–553.

Ludwig,J., Terlau,H., Wunder,F., Brüggemann,A., Pardo,L.A., Marquardt,A., Stühmer,W. and Pongs,O. (1994) Functional expression of a rat homologue of the voltage gated *ether à go-go* potassium channel reveals differences in selectivity and activation kinetics between the *Drosophila* channel and its mammalian counterpart. *EMBO J.*, **13**, 4451–4458.

Mauro,T., Dixon,D.B., Komuves,L., Hanley,K. and Pappone,P.A. (1997) Keratinocyte K^+ channels mediate Ca^{2+}-induced differentiation. *J. Invest. Dermatol.*, **108**, 864–870.

McClelland,A., Kuhn,L.C. and Ruddle,F.H. (1984) The human transferrin receptor gene: genomic organization and the complete primary structure of the receptor deduced from a cDNA sequence. *Cell*, **39**, 267–274.

Meyer,R. and Heinemann,S.H. (1998) Characterization of an *eag*-like potassium channel in human neuroblastoma cells. *J. Physiol.*, **508**, 49–56.

Mosmann,T. (1983) Rapid colorimetric assay for cellular growth and survival: application to proliferation and cytotoxicity assays. *J. Immunol. Methods*, **65**, 55–63.

Nilius,B. and Wohlrab,W. (1992) Potassium channels and regulation of proliferation of human melanoma cells. *J. Physiol.*, **445**, 537–548.

Occhiodoro,T., Bernheim,L., Liu,J.H., Bijlenga,P., Sinnreich,M., Bader,C.R. and Fischer-Lougheed,J. (1998) Cloning of a human *ether-à-go-go* potassium channel expressed in myoblasts at the onset of fusion. *FEBS Lett.*, **434**, 177–182.

Pappas,C.A. and Ritchie,J.M. (1998) Effect of specific ion channel blockers on cultured Schwann cell proliferation. *Glia*, **22**, 113–120.

Pappone,P.A. and Ortiz-Miranda,S.I. (1993) Blockers of voltage-gated K^+ channels inhibit proliferation of cultured brown fat cells. *Am. J. Physiol.*, **264**, C1014–C1019.

Pardo,L.A., Brüggemann,A., Camacho,J. and Stühmer,W. (1998) Cell cycle-related changes in the conducting properties of r-eag K^+ channels. *J. Cell Biol.*, **143**, 767–775.

Richter,G., Kruger-Krasagakes,S., Hein,G., Huls,C., Schmitt,E., Diamantstein,T. and Blankenstein,T. (1993) Interleukin 10 transfected into Chinese hamster ovary cells prevents tumor growth and macrophage infiltration. *Cancer Res.*, **53**, 4134–4137.

Robertson,G.A., Warmke,J.W. and Ganetzky,B. (1996) Potassium currents expressed from *Drosophila* and mouse *eag* cDNAs in *Xenopus* oocytes. *Neuropharmacology*, **35**, 841–850.

Rouzaire-Dubois,B. and Dubois,J.M. (1998) K^+ channel block-induced mammalian neuroblastoma cell swelling—a possible mechanism to influence proliferation. *J. Physiol.*, **510**, 93–102.

Santella,L. (1998) The role of calcium in the cell cycle: facts and hypotheses. *Biochem. Biophys. Res. Commun.*, **244**, 317–324.

Schneider,C., Owen,M.J., Banville,D. and Williams,J.G. (1984) Primary structure of human transferrin receptor deduced from the mRNA sequence. *Nature*, **311**, 675–678.

Skryma,R.N., Prevarskaya,N.B., Dufy-Barbe,L., Odessa,M.F., Audin,J. and Dufy,B. (1997) Potassium conductance in the androgen-sensitive prostate cancer cell line, LNCaP: Involvement in cell proliferation. *Prostate*, **33**, 112–122.

Soto,F., García-Guzmán,M., Gómez-Hernández,J.M., Hollmann,M., Karschin,C. and Stühmer,W. (1996) $P2X_4$: an ATP-activated ionotropic receptor cloned from rat brain. *Proc. Natl Acad. Sci. USA*, **93**, 3684–3688.

Stein,G.S., Stein,J.L., Lian,J.B., Last,T.J., Owen,T. and McCabe,L. (1995) Cell synchronization as a basis for investigating control of proliferation in mammalian cells. In Studzinski,G.P. (ed.), *Cell Growth and Apoptosis. A Practical Approach.* IRL Press, Oxford, UK, pp. 193–203.

Strobl,J.S., Wonderlin,W.F. and Flynn,D.C. (1995) Mitogenic signal transduction in human breast cancer cells. *Gen. Pharmacol.*, **26**, 1643–1649.

Suessbrich,H., Waldegger,S., Lang,F. and Busch,A.E. (1996) Blockade of HERG channels expressed in *Xenopus* oocytes by the histamine receptor antagonists terfenadine and astemizole. *FEBS Lett.*, **385**, 77–80.

Terlau,H., Ludwig,J., Steffan,R., Pongs,O., Stühmer,W. and Heinemann,S.H. (1996) Extracellular Mg^{2+} regulates activation of rat eag potassium channel. *Pflügers Arch.*, **432**, 301–312.

Wagner,R.W. (1994) Gene inhibition using antisense oligonucleotides. *Nature*, **372**, 333–335.

Warmke,J.W. and Ganetzky,B. (1994) A family of potassium channel genes related to *eag* in *Drosophila* and mammals. *Proc. Natl Acad. Sci. USA*, **91**, 3438–3442.

Warmke,J., Drysdale,R. and Ganetzky,B. (1991) A distinct potassium channel polypeptide encoded by the *Drosophila eag* locus. *Science*, **252**, 1560–1562.

Woodfork,K.A., Wonderlin,W.F., Peterson,V.A. and Strobl,J.S. (1995) Inhibition of ATP-sensitive potassium channels causes reversible cell-cycle arrest of human breast cancer cells in tissue culture. *J. Cell Physiol.*, **162**, 163–171.

Received May 31, 1999; revised August 10, 1999; accepted August 24, 1999